Available online at www.eccomasproceedia.org
Eccomas Proceedia COMPDYN (2023) 4286-4298

ECCOMAS
Proceedia

COMPDYN 2023
9th ECCOMAS Thematic Conference on
Computational Methods in Structural Dynamics and Earthquake Engineering
M. Papadrakakis, M. Fragiadakis (eds.)
Athens, Greece, 12-14 June 2023

GROUND MOTION PROCESSING IN ROCKING STRUCTURES

Medhat Elmorsy[1, 2] and Michalis F. Vassiliou[1]

[1]Chair of Seismic Design and Analysis, Institute of Structural Engineering (IBK), ETH Zürich

[2]Structural Engineering Department, Mansoura University, Mansoura, Egypt

{medhat.elmorsy, vassiliou}@ibk.baug.ethz.ch

Abstract

Recorded ground motions require filtering and baseline correction to remove noise that results in unrealistic velocity and displacement time histories. The effect of ground motion processing is well studied for elastic and inelastic oscillators; however, it has not been studied for the rocking oscillator. The behavior of the rocking oscillator is used to describe a wide range of systems; such as masonry structures, unanchored equipment, and ancient Greco Roman and Chinese temples. This paper investigates the effect of ground motion processing on the response of the rocking oscillator. Different types of digital ground motions (pulse like and non pulse like) and different processing schemes and scheme parameter values are presented to illustrate this effect on the displacement spectra for planar rocking blocks. Based on the results of this paper, on a single ground motion basis, ground motion processing has an effect on the rocking spectra which is basically similar to the elastic oscillator. However, when treating the problem in a statistical way (by comparing the statistics of the response to sets of ground motions, not to a single ground motion - as seismic design typically requires), the effect is significantly reduced. In fact, as long as the system is not close to overturning (failure), the rocking spectra only loosely depend on the processing scheme.

Keywords: Near-field ground motions, Ground motion processing, Rocking, Digital filtering, Uplifting structures.

ISSN:2623-3347
Peer-review under responsibility of the organizing committee of COMPDYN 2023.
doi: 10.7712/120123.10718.20776

1 INTRODUCTION

Starting with Housner's seminal paper in 1963 [1], the study of the rocking oscillator has gained an increasing attention due to its ability to describe a wide range of systems that cannot be adequately described by the elastic oscillator [2-12]. Moreover, rocking motion can be used as a seismic isolation mechanism [13-19]. Interestingly, rocking has been used since more than 40 years as a seismic isolation method in the former USSR countries via intentionally designing a soft rocking story that limits the force transmitted to the super structure [20].

The use of ground motion records for time history analysis is a cornerstone in earthquake engineering. However, these recorded motions are often plagued by diverse sources of noise. Noise can be defined as any distortion in the record that lead to physically unrealistic velocity or displacement traces. The velocity trace should show zero values at the end of the record. On the other hand, the displacement trace should reflect the residual displacement (often referred to as the fling step) at the recording site, acquired from geodetic data. Practically, many ground motion processing schemes (including the procedure adopted by the widely-used NGA West 2 [21] ground motion database) neglect the effect of the fling step, mainly due to the lack of geodetic data or lack of interest in the fling step effect (e.g., in the case of far-field motions). Therefore, the use of processing and noise filtration schemes is inevitable.

Processing of strong ground motions typically starts with removing the mean value of the pre-event buffer (or the mean of the whole record in case pre-event data are not available, which is the case in analog ground motion records). The next step, which is the essential part, is to apply a low and high pass Butterworth filters, of which, the most important is the high-pass filter (low-cut filter) which aims to remove the long period noise that exists in both analog and digital records. Two types of digital filters are typically used; causal and acausal (zero-phase) filters. Causal filters result in shifted filtered ground motion signal in contrary to acausal filters. Acausal filters is the state of the art within ground motion processing context. NGA West 1 project used causal filtered ground motions, while acausal filters were used in the updated version of the project, NGA West 2 [21]. Moreover, the use of time domain baseline corrections is often combined with the use of filters. The choice of filter parameters (order and corner frequency) involves some degree of subjective judgement since the noise source is not well understood, especially the long period noise [22]. Boore and Bommer [22] claimed that there is no way to identify a best processing technique for an individual ground motion and that the uncertainty of the whole procedure should be appreciated by the end users of the processed record.

In this study, a procedure based on the procedure adopted by PEER NGA West 2 database was implemented with variations in the low-cut filter corner frequency. The variations in the cut-off frequency, being the most important parameter in ground motion processing, are aimed at simulation of the uncertainty and subjectivity in that choice. In addition, the effect of filter causality is also discussed. These variations of ground motion filtering are used to quantify the effect of ground motion processing on the response of rocking structures. As a proxy for understanding the behavior of rocking structures, the rocking displacement spectra is used, as discussed in Section 2 of this paper.

2 ROCKING DISPLACEMENT SPECTRA

This section briefly describes the rocking oscillator and underline some of its properties that will facilitate the study of the dependence of its response on ground motion correction methods. The equation of in-plane motion for a rigid rectangular rocking block (Figure 1a) with slenderness ratio α and a semi-diagonal length R is:

$$\ddot{\theta} = -p^2(\sin[\pm\alpha - \theta] + \frac{\ddot{u}_g}{g}\cos[\pm\alpha - \theta]) \quad (1)$$

where $p = \sqrt{(3g)/(4R)}$ is the frequency parameter of the rocking column. The upper and the lower sign in front of α corresponds to a positive and a negative rocking angle θ, respectively, with respect to the defined coordinate system in Figure 1a. It is assumed that energy is only dissipated during impact. Housner [1] assumed that (a) the impact is instantaneous and (b) the impact forces are concentrated on the impacting corner (Point O in Figure 1a). Based on these assumptions, the ratio of post to pre-impact rotational velocities (coefficient of restitution) is:

$$r = 1 - \frac{3}{2}\sin^2\alpha \quad (2)$$

Inspecting equation (1), one can conclude that the rotational response of a rocking block to a given ground motion is a function of α and R. Similarly, for the elastic oscillator, the response is a function of the eigen period, T, and damping ratio ζ [23]. One difference between the rocking and the elastic oscillator is that in the case of the former, both R and α strongly influence the rotational response whereas in the latter one parameter (T) is more influential than the other (ζ). Manzo and Vassiliou [23] suggested that using displacement response instead of rotational response will further reduce the dimensionality of the rocking oscillator problem. The top displacement, u, of the rocking block can be obtained by a one-to-one mapping of rotation, θ, (see Figure 1a):

$$u = 2R\sin(\pm\alpha) - 2R\sin(\pm\alpha - \theta) \quad (3)$$

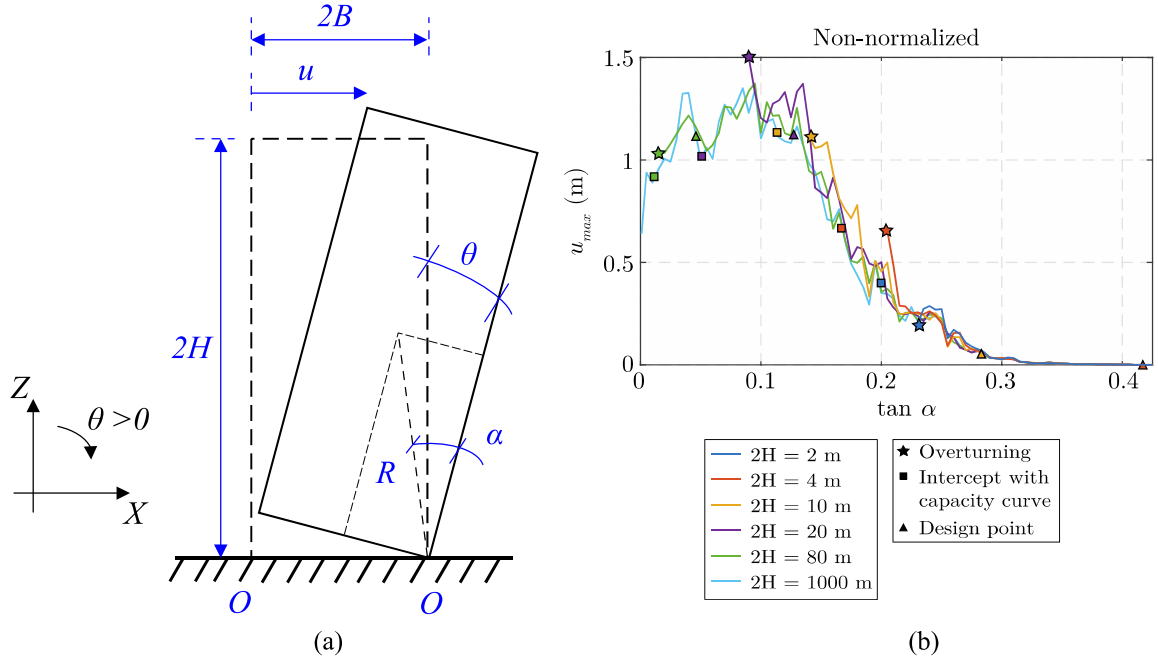

Figure 1: Displacement-based analysis of rocking blocks: (a) geometry of the rigid rocking block showing angle of rotation (θ) and horizontal displacement (u) (b) median rocking displacement spectra median for different sizes for a set of near-field pulse-like records [23].

They concluded that a large and a small rocking block of the same slenderness will have the same top displacement, given that both are away from overturning (they named this conclusion:

"*equal displacement rule of rocking structures*"). They obtained the same result using analytical pulses and actual ground motion records (FEMA P695 [24] ground motion sets) as input excitations. The condition that the blocks are not close to overturning is a design requirement, so practically, slenderness is the only parameter affecting the displacement response, not the block size. Vassiliou et al. [25] have proven that rigid rocking blocks with the same height (H) attached to massless foundations of the same size behave identically, no matter what their actual column width is. Therefore, it is more meaningful to use H as a size parameter instead of R, even if the former does not explicitly appear in the equation of motion. Figure 1b depicts the median rocking displacement spectra for different sizes (expressed in terms of height $2H$) for a set of near-field pulse-like records. The rocking spectrum throughout this paper refers to the relationship between the tangent of the slenderness angle on the horizontal axis and the maximum displacement response due to the ground excitation on the vertical axis. The figure shows the equal displacement rule and also shows some deviation when the block is near overturning (see block with size $2H = 20$ m).

Accordingly, in this paper, a block with height ($2H$) of 2000 meters was used to study the effect of different processing/filtering variations on the displacement response of rocking structures. A height of 2000 m represent the case when $2H \rightarrow \infty$ which is being studied for mathematical completeness (having spectrum ordinates at very low tangent of the slenderness angle).

3 GROUND MOTIONS SELECTION

In total, 12 digital ground motions were selected and split into two groups (near field pulse-like and near field non pulse-like) as described in FEMA P695 [24]. The nature of noise and baseline tilts in analog records are very distinct from digital records [22]. A discussion of this different nature is offered in [22, 26]. In digital records, the velocity trace noise typically appears to have a linearly increasing baseline offset. This paper focuses on digital records.

A source-site distance (defined as the Joyner-Boore distance [27]) of 10 km was used to separate near- and far-field records. Only strong motions (magnitude > 6.5) were considered. For each ground motion, the two horizontal components were treated as different records, resulting in 24 records in total. The vertical component of the ground motion was not used in this study, as it seems that it does not significantly influence the response of the rocking oscillator [28, 29]. The ground motions were classified as pulse- or non pulse-like based on the classification of PEER NGA West 2 database, if the ground motion is available there. Otherwise, the methodology and the code developed by [30, 31] are used to classify the records.

Tables 1 summarizes the ground motion database. The PGA, PGV, and PGD values in Tables 1 and 2 are calculated using the records corrected using acausal filtering (discussed later in the paper) with a high-pass filter corner frequency 0.1 Hz. These values are taken as the maximum of the temporal maximum of each of the two horizontal components of each record, i.e. $PGA=\max(PGA_x,PGA_y)$.

4 GROUND MOTION PROCESSING PARAMETERS

The adopted processing scheme comprised a baseline correction and an application of a causal or acausal filter. Figure 2 depicts the adopted processing schemes for acausal filtering. The scheme was based on the NGA West 2 processing methodology [21, 32]. It starts by removing the pre-event buffer mean. Then the start and the end of the signal are tapered using cosine tapers with a length equal to 1% of the trace length [33]. The next step is to apply zero pads at the end of the record so that the number of points in the time series is a power of two since the filtering is conducted in the frequency-domain using the Fast Fourier transform (FFT) [34].

Event	*M*	Station	Network	R_{jb} (km)	PGA (m/s^2)	PGV (m/s)	PGD (m)	Pulse/No-Pulse
2008 Wenchuan, China	7.90	Mianzuqing-ping	NSMONS[1]	0.00	7.127	0.905	0.565	Pulse-like
1999 Chi-Chi, Taiwan	7.62	TCU049	TSMIP[2]	3.76	2.658	0.625	0.348	Pulse-like
		TCU068	TSMIP	0.00	5.014	1.560	1.401	Pulse-like
		TCU102	TSMIP	1.49	2.909	0.829	0.728	Pulse-like
		TCU082	TSMIP	5.16	2.119	0.431	0.378	Pulse-like
		TCU065	TSMIP	0.57	7.750	1.158	0.710	Pulse-like
2016 Kaikoura	7.80	KEKS	GeoNet[3]	3.00	10.909	1.054	0.453	No-pulse
		WDFS	GeoNet	8.50	12.232	0.922	0.348	No-pulse
		WTMC	GeoNet	0.70	10.345	1.064	0.367	No-pulse
2015 Nepal	7.80	KATNP	CESMD[4]	0.10	1.655	0.983	0.843	No-pulse
2016 Kumamoto	7.00	KMM004	K-NET, KiK-net, and JMA[5]	3.90	3.439	0.777	0.457	No-pulse
		KMMH16		0.50	11.574	1.343	0.455	No-pulse

[1]NSMONS: National Strong-Motion Observation Network System of China.
[2]TSMIP: Taiwan Strong Motion Instrumentation Program.
[3] GeoNet: The New Zealand GeoNet project.
[4]CESMD: Center for Engineering Strong Motion Data [35], with stations that belong to different networks including coast and geodetic survey (C&GS), California Strong Motion Instrumentation Program (CSMIP), and United States National Strong-Motion Network (NSMP).
[5]K-NET, KiK-net: Japan network of strong-motion seismographs, JMA: Japan Meteorological Agency.

Table 1: Details of the selected digital records used in this paper.

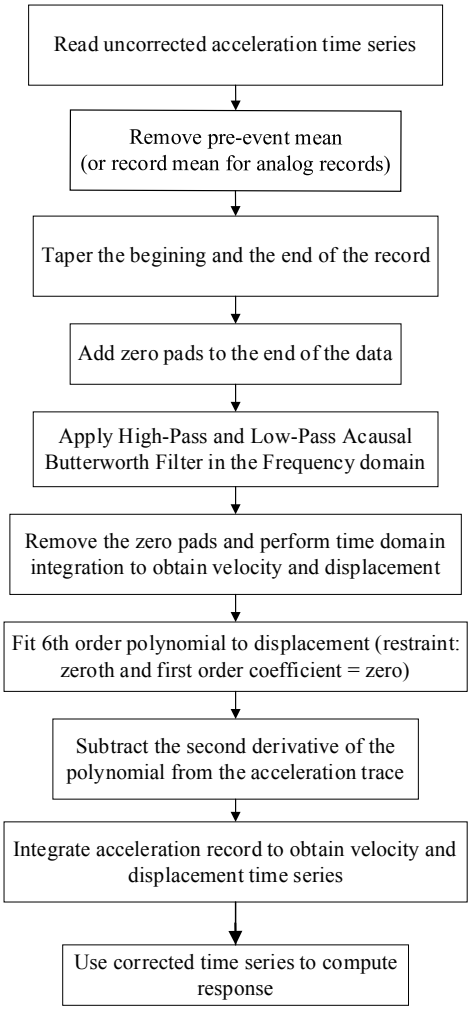

Figure 2: The adopted processing algorithm for acausal filtering based on the PEER NGA West 2 processing scheme [21, 32].

Thereafter, high pass and low pass acausal Butterworth filters are applied to the acceleration time series in the frequency domain. Then, the zero pads are removed and a 6th order polynomial is fitted to the displacement trace (obtained by double integration of the acceleration trace) and the second derivative of the polynomial is subtracted from the acceleration time history. A similar procedure was used for the causal filtering scheme with a causal Butterworth filter (Figure 3). For causal filters the tapering and zero padding steps are not included since they are only needed for the acausal filtering [32, 36].

Apart from the baseline correction and filtering, the time series for all ground motion records were checked for non-standard noise (e.g., unrealistic spikes) on a single record basis. The MATLAB code used in this study was based on the codes of Akkar [21, 32] and Abrahamson [32]. The used corner periods of the high-pass filters were 10, 15, 20, 30, 40, and 60 seconds, with longer periods corresponding to more relaxed filtering and shorter periods corresponding to more intense filtering. The chosen high-pass corner periods range was based on [37] in which the effects of long-period processing on structural collapse predictions of steel moment frames was investigated. The low-pass filter (causal and acausal) corner frequency was chosen to be 25 Hz (i.e. corner period equal to 0.04 seconds).

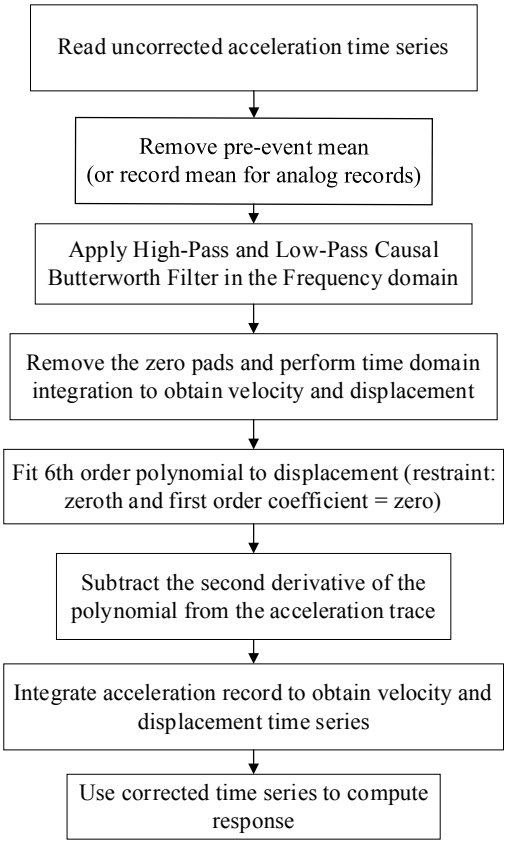

Figure 3: The adopted processing algorithm for causal filtering.

Figure 4 shows the filter frequency response function (magnitude and phase) for the adopted causal and acausal (zero phase) filters with 8 poles for different cut-off periods. The figure depicts the difference in phase shifts between causal and acausal filters as discussed earlier. It is also worth mentioning that discussions about usable spectral periods (often expressed relative to the filter corner period) are irrelevant to the rocking oscillator since its "period" is amplitude dependent and can take values from zero to infinity [1]. Verification of the adopted processing

scheme is presented in [26]. Notably, in this study, the Zero Order Corrected (ZOC) record refers to the record with mean removed (mean of the pre-event portion as discussed earlier).

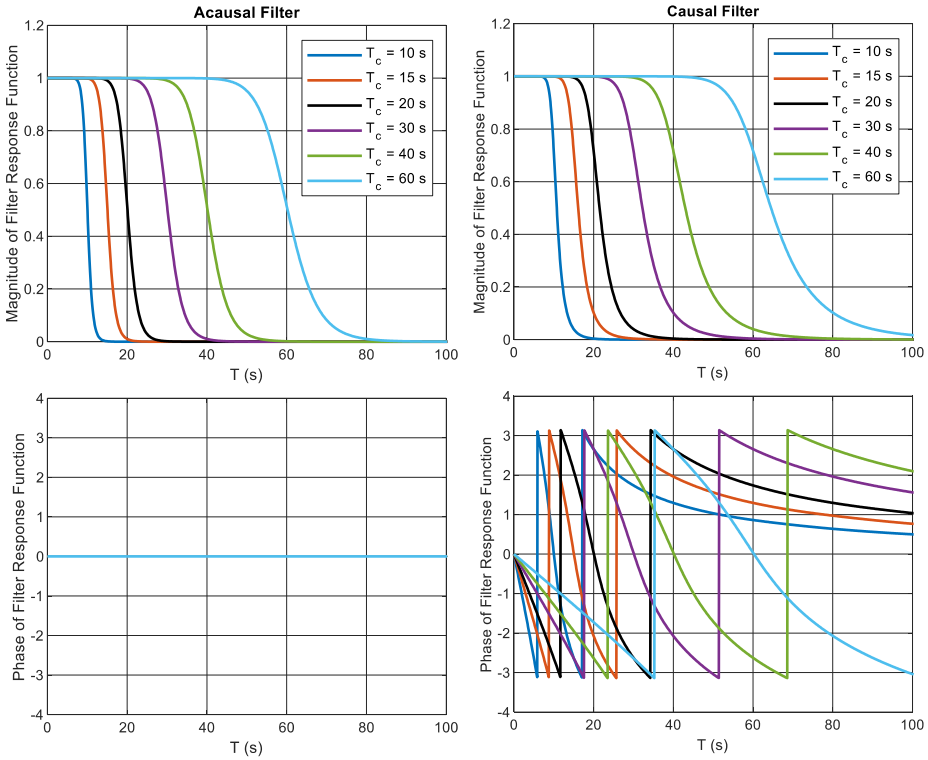

Figure 4: Filter response function (magnitude and phase in radian) of the adopted acausal (zero phase) and causal high-pass filters (number of poles = 8).

5 RESULTS

As discussed earlier, the rocking spectra presented in this study plot the maximum top displacement of a rigid block versus the tangent of the slenderness angle. Accordingly, the rocking spectrum is not to be confused with the linear elastic oscillator spectrum (elastic spectrum). The rocking spectrum is highly non-linear and is not correlated to the elastic spectrum [7]. For reasons that will be discussed later in this section, all ground motions were scaled to have a PGV of 50 cm/s. As the raw ground motion results in unrealistically high PGVs, the scaling factor for different corner periods and for the same component was kept constant and equal to the one needed to scale the record that was processed with the 10 seconds cut off period and an acausal filter to a PGV of 50 cm/s. As the number of analyses was high, the ETH Zurich scientific computing cluster (Euler) was used for performing the analysis.

Figure 5 shows some indicative rocking spectra for causal and acausal filtering. To develop Figure 5, the recordings at the following stations were used: El Centro for El Mayor Cucapah earthquake and WTMC for Kaikoura earthquake. One can observe that causal filtering resulted in higher variability than acausal filtering, an observation that agrees with previous studies for elastic systems [36]. In addition, in all cases in Figure 5, the variability of the spectrum due to the choice of different cut-off frequencies decreases with increasing tangent of the slenderness angle α. There is a physical reason for this: As the slenderness angle decreases, the rocking

block tilts to larger angles. Larger tilt angles lead to larger periods [1], where the variability due to high-pass filtering typically is expected to increase, as in elastic systems [36].

The discussion up till this point only focused on the spectra on a single ground motion basis. As rocking is a very sensitive problem to all the parameters that define it, Yim et al. [38], as early as 1980, have suggested that a sensitivity analysis of the rocking oscillator should be performed in a statistical sense, namely by comparing the statistics of the response to an ensemble of ground motions, rather than to individual excitations [39]. Such a statistical approach is not only applied to rocking structures: Riddell and Newmark [40] produced inelastic spectra for yielding structures based on statistics on ensembles of excitations. In fact, this approach is consistent with the fundamental seismic design problem, which involves computing the response to a set of ground motions, rather than to an individual one [41, 42].

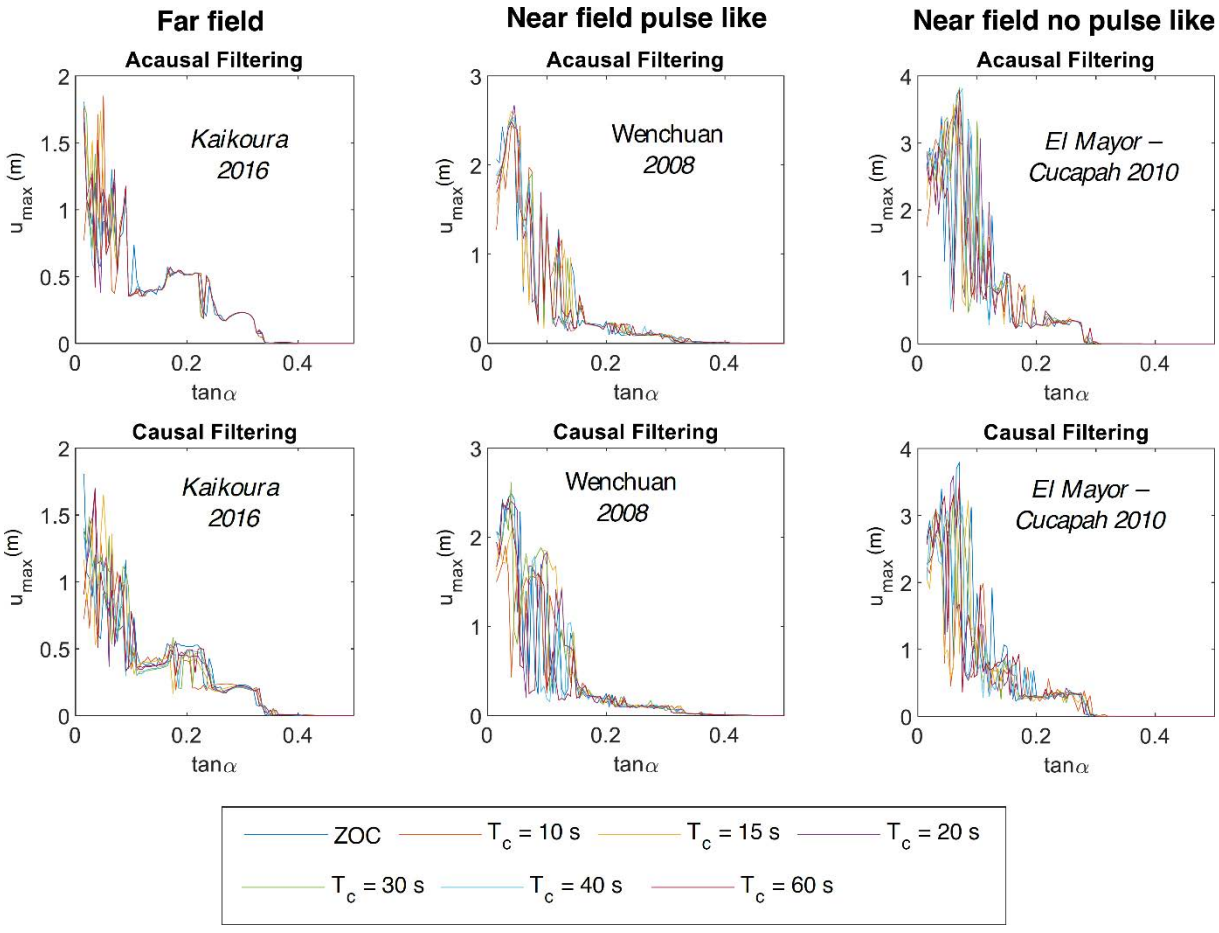

Figure 5: Example rocking spectra for different categories of filtering schemes and ground motions for digital ground motion records (left: far field, middle: near field pulse like, right: near field non pulse-like).

For an ensemble of ground motions to be useful, in this paper all ground motions were scaled to the same PGV. PGV was used as an intensity measure, as it performs better than PGA or PGD for rocking structures [43, 44].

Figures 6 and 7 show the median rocking spectra for the near-field pulse-like and near-field non pulse-like record bins, derived for different processing schemes. As stated earlier, all the rocking spectra in this paper are derived for size (2H) of 2000 meters which represent the case when $2H \rightarrow \infty$ that is being studied for mathematical completeness. Then, these rocking spectra

could be used to determine the response of rocking blocks of finite size. Moreover, Figures 6 and 7 show the 95% confidence interval of the median (over the ground motions of each set) response for the zero-order corrected case (ZOC), i.e. of the case were only the mean of the record was removed. The 95% confidence interval (CI) was constructed using the bootstrap method [45] by taking 1000 response samples for each value of tanα. Taking 10,000 response samples did not seem to change the CIs.

Based on the median rocking spectra (Figures 6 and 7), one can observe that for larger tanα (resulting into smaller displacements) the rocking spectra only loosely depend on the processing scheme, as it can also be observed on an individual motion base (Figure 5). For smaller tanα, there seems to be some non-negligible influence of the response on the processing scheme, but in most cases, the curves for the different processing schemes fall within the 95% confidence interval of the rocking spectrum of the zero-order corrected (ZOC) case, indicating that the motion-to-motion variability is larger than the variability caused by the different correction schemes. Moreover, there is not trend of the response with respect to increasing or decreasing corner period or with respect to causal or acausal filtering. Therefore, even if the different processing schemes do influence the rocking response, the bias of this influence seems negligible – at least for the parameter values examined. The above conclusion seems to be independent of whether the ground motion is pulse like or non pulse like.

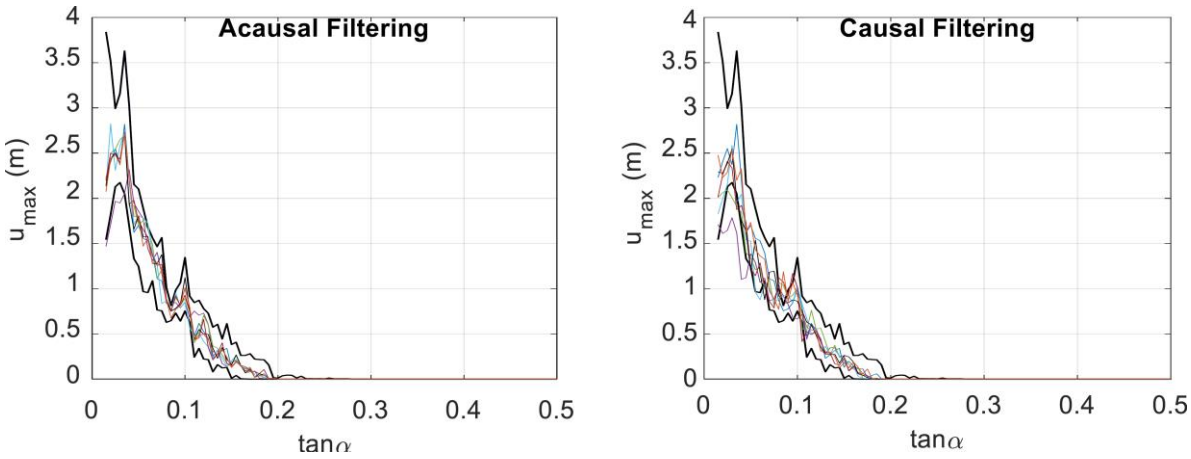

Figure 6: Median estimates of the rocking spectra for different correction schemes for the near-field pulse-like record set (the confidence interval is derived for the ZOC spectrum).

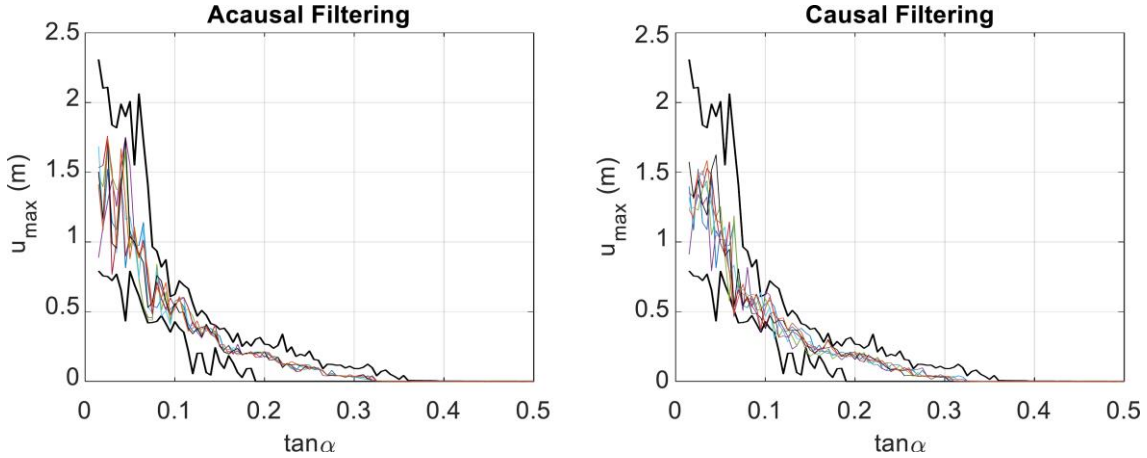

Figure 7: Median estimates of the rocking spectra for different correction schemes for the near-field non pulse-like record set (the confidence interval is derived for the ZOC spectrum).

Figure 8 shows the standard deviation and the coefficient of variation (COV, calculated as the standard deviation divided by the mean value) of the median estimates of the rocking spectra (Figures 6 and 7) for the cases presented in this study. The standard deviation values decrease for all the cases with increasing tanα, confirming that the variability decreases with tanα. For higher tangent of the slenderness angle, the COV reaches large values (on the order of 250%), but this only because in this region the mean tends to zero. Notably, for all the cases, the COV for the lower values of the tangent of the slenderness angle had almost a constant value of less than 0.2 on average.

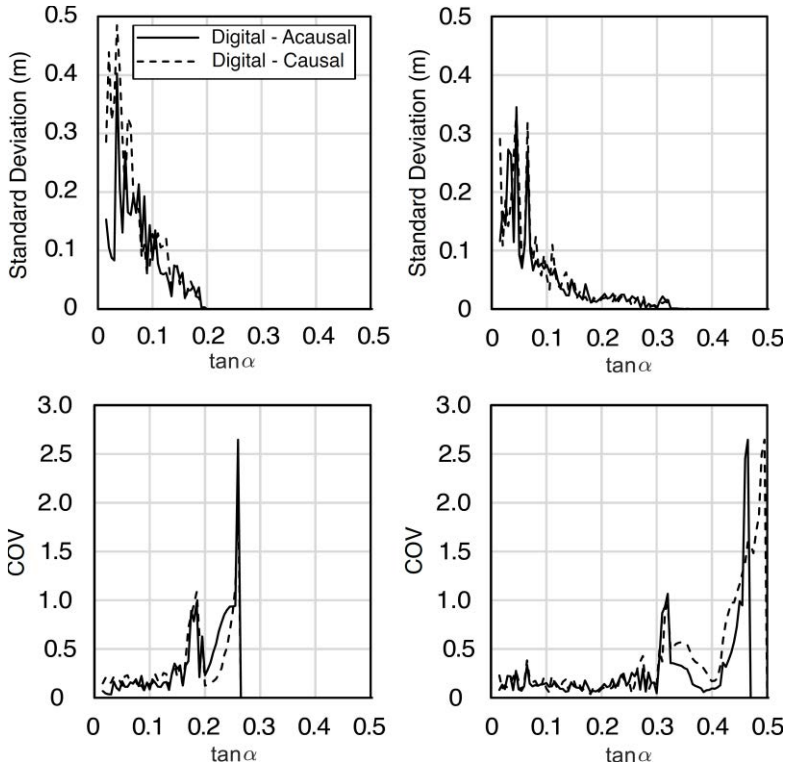

Figure 8: Variability (standard deviation and coefficient of variation) of the median estimates of the rocking spectra for different processing schemes derived for the studies sets of ground motions (left: near field pulse like, right: near field non pulse-like).

6 CONCLUSIONS

This paper studies the influence of ground motion filtering on the response of the rocking isolator. To this end, different kinds of ground motions and variations of processing schemes were used to explore their effect on the rocking displacement spectra for planar rocking blocks. On a single ground motion basis, it can be concluded that:

- Causal filtering results in higher variability than acausal filtering; agreeing with previous studies on the elastic oscillator.
- The variability of the spectrum due to the choice of different cut-off frequencies decreases with increasing tangent of the slenderness angle.

However, the seismic design problem does not involve the response to an individual ground motion but the statistics of the responses to a set of ground motions that characterize the seismic hazard. Therefore, this paper has argued that the influence of processing schemes should be evaluated statistically, essentially by evaluating whether they induce bias in the spectra. This work followed such an approach and showed that the median rocking displacement spectra to sets of ground motions are not significantly sensitive to the ground motion processing scheme.

In most cases, the curves for the different processing schemes fall within the 95% confidence interval of the rocking spectrum of the zero-order corrected (ZOC) case. Therefore, the motion-to-motion variability was more important than the processing scheme. This conclusion holds for filter cut off periods larger than or equal to 10 seconds and applies to both causal and acausal filters, and to all near field pulse like and near field non pulse like records.

ACKNOWLEDGEMENTS

This work was supported by the ETH Zurich under grant ETH-11 21-1.

REFERENCES

[1] G.W. Housner. The behavior of inverted pendulum structures during earthquakes. *Bull Seismol Soc Am*. 1963; 53(2): 403-417.

[2] A.K. Chopra, S.C-S. Yim. Simplified earthquake analysis of structures with foundation uplift. *J Struct Eng*. 1985; 111(4): 906-930.

[3] I.N. Psycharis. Effect of base uplift on dynamic response of SDOF structures. *J Struct Eng*. 1991; 117(3): 733-754.

[4] G. Oliveto, I. Calio, A. Greco. Large displacement behaviour of a structural model with foundation uplift under impulsive and earthquake excitations. *Earthq Eng Struct Dyn*. 2003; 32(3): 369-393.

[5] D. D'Angela, G. Magliulo, E. Cosenza. Seismic damage assessment of unanchored non-structural components taking into account the building response. *Structural Safety*. 93, 102126, 2021. https://doi.org/10.1016/j.strusafe.2021.102126

[6] D. D'Angela, G. Magliulo, E. Cosenza. Towards a reliable seismic assessment of rocking components. *Engineering Structures*. 230, 111673. 2021. https://doi.org/10.1016/j.engstruct.2020.111673

[7] A.I. Giouvanidis, E.G. Dimitrakopoulos, P.B. Lourenço. Chattering: an overlooked peculiarity of rocking motion. *Nonlinear Dynamics*. 109, 459–477. 2022

[8] M. Kohrangi, K. Bakalis, G. Triantafyllou, D. Vamvatsikos, P. Bazzurro. Hazard consistent record selection procedures accounting for horizontal and vertical components of the ground motion: Application to liquid storage tanks. *Earthquake Engng Struct Dyn*. 2023;52:1232–1251.https://doi.org/10.1002/eqe.3813

[9] J. Wang, W. Chen, K. Dai, T. Li, S. Tesfamariam, Y. Lu. Seismic damage evaluation of unanchored nonstructural components under combined effects of horizontal and vertical near-fault ground motions. *Earthquake Engng Struct Dyn*. 2023;1-21.https://doi.org/10.1002/eqe.3846

[10] Q.T.M Ma. The mechanics of rocking structures subjected to ground motion. 2010, ResearchSpace@ Auckland.

[11] S. Acikgoz, M.J. DeJong. The interaction of elasticity and rocking in flexible structures allowed to uplift. *Earthq Eng Struct Dyn*. 2012; 41(15): 2177-2194.

[12] N. Makris, D. Konstantinidis. The rocking spectrum and the limitations of practical design methodologies. *Earthq Eng Struct Dyn*. 2003; 32(2): 265-289.

[13] S.I. Reyes, J.L. Almazán. A novel device for a vertical rocking isolation system with uplift allowed for industrial equipment and structures. *Engineering Structures*. 2020; 214:110595.

[14] K. Zhang, J. Junfeng, L. Ning, j. Zhao, Y. Bai. Analytical model for evaluating lateral force capacity of precast concrete-filled steel tube column. *Engineering Structures*. https://doi.org/10.1016/j.engstruct.2022.115106

[15] S. Li, H-Ho. Tsang, N. Lam. Seismic protection by rocking with superelastic tendon restraint. *Earthquake Engng Struct Dyn*. 2022; 51:1718–1737. https://doi.org/10.1002/eqe.3635

[16] J. Yang, Z. Yang, Y. Chen, Y. Lv, N. Chouw. Finite element simulation of an upliftable rigid frame bridge under earthquakes: Experimental verification. *Soil Dynamics and Earthquake Engineering*. 2023. https://doi.org/10.1016/j.soildyn.2022.107716

[17] C.G. Lachanas, D. Vamvatsikos, E.G. Dimitrakopoulos. Intensity measures as interfacing variables versus response proxies: The case of rigid rocking blocks. *Earthquake Engng Struct Dyn*. 2023;1-18.https://doi.org/10.1002/eqe.3838

[18] C.G. Lachanas, D. Vamvatsikos, E.G. Dimitrakopoulos. Statistical property parameterization of simple rocking block response. *Earthquake Engineering and Structural Dynamics*. 2023;52:394-414. https://doi.org/10.1002/eqe.3765

[19] S.I. Reyes, J.L. Almazán, M.F. Vassiliou, N.F. Tapia, J.I. Colombo, J.C. de la Llera. Full‐scale shaking table test and numerical modeling of a 3000‐liter legged storage tank isolated with a vertical rocking isolation system. *Earthquake Engineering & Structural Dynaics*. 2022;51(6):1563-85.

[20] J. Bachmann, M.F. Vassiliou, B. Stojadinović. Dynamics of rocking podium structures. Earthquake Engineering & Structural Dynamics. 2017. 46(14): p. 2499-2517.

[21] T.D. Ancheta, R.B. Darragh, J.P. Stewart, E. Seyhan, W.J. Silva, B.S-J. Chiou, K.E. Wooddell, R.W. Graves, A.R. Kottke, D.M. Boore, T. Kishida, J.L. Donahue. *PEER NGA-West2 Database*. 2013; Pacific Earthquake Engineering Research Center, University of California, Berkeley, CA. p. 134.

[22] D.M. Boore, J.J. Bommer. Processing of strong-motion accelerograms: needs, options and consequences. *Soil Dyn Earthquake Eng*. 2005; 25(2): 93-115.

[23] N. Reggiani Manzo, M.F. Vassiliou. Displacement-based analysis and design of rocking structures. *Earthq Eng Struct Dyn*. 2019; 48(14): 1613-1629.

[24] FEMA P695. *Quantification of Building Seismic Performance Factors*. Washington, D.C: Rep. FEMA P695, Federal Emergency Management Agency; 2009.

[25] M.F. Vassiliou , K.R. Mackie, B. Stojadinović. Dynamic response analysis of solitary flexible rocking bodies: modeling and behavior under pulse‐like ground excitation. *Earthquake engineering & structural dynamics*. 2014. **43**(10): p. 1463-1481.

[26] M. Elmorsy, M.F. Vassiliou . Effect of ground motion processing and filtering on the response of rocking structures. *Earthquake Engineering & Structural Dynamics*. 2023.

[27] N.A. Abrahamson, K.M. Shedlock. Overview. *Seismological Research Letters*. 1997; 68(1): 9-23.

[28] C.G. Lachanas, D. Vamvatsikos, M.F. Vassiliou. The influence of the vertical component of ground motion on the probabilistic treatment of the rocking response of free-standing blocks. *Earthq Eng Struct Dyn*. 202; 51(8): 1874-1894.

[29] N. Makris, G. Kampas, Size Versus Slenderness: Two Competing Parameters in the Seismic Stability of Free‐Standing Rocking Columns Size Versus Slenderness: Two Competing Parameters in the Seismic Stability of Free‐Standing Rocking Columns. *Bulletin of the Seismological Society of America*, 2016. 106(1): p. 104-122.

[30] S.K. Shahi, J.W. Baker. An efficient algorithm to identify strong-velocity pulses in multicomponent ground motions. *Bull Seismol Soc Am*. 2014; 104(5): 2456-2466.

[31] S.K. Shahi, J.W. Baker . *Pulse classification algorithm*. 2012. http://www.jackwbaker.com/pulse-classification.html (last accessed 2nd December 2022).

[32] D.M. Boore, A. Azari Sisi, S. Akkar. Using pad-stripped acausally filtered strong-motion data. *Bull Seismol Soc Am*. 2012; 102(2): 751-760.

[33] C.A. Goulet, et al. PEER NGA-east database. *Earthquake Spectra*. 2021. 37(1_suppl): p. 1331-1353.

[34] D.M. Boore. On pads and filters: Processing strong-motion data. *Bull Seismol Soc Am*. 2005; 95(2): 745-750.

[35] CESMD, Center for Engineering Strong-Motion Data (CESMD) https://www.strongmotioncenter.org/ (last accessed 2nd December 2022).

[36] D.M. Boore, S. Akkar. Effect of causal and acausal filters on elastic and inelastic response spectra. *Earthq Eng Struct Dyn*. 2003; 32(11): 1729-1748.

[37] K. Buyco, B. Roh, T.H. Heaton. Effects of long-period processing on structural collapse predictions. *Earthquake Spectra*. 2021; 37(1): 204-234.

[38] C.S. Yim, A.K. Chopra, J. Penzien. Rocking response of rigid blocks to earthquakes. *Earthq Eng Struct Dyn*. 1980; 8(6): 565-587.

[39] A.A. Katsamakas, M.F. Vassiliou. Finite element modeling of free‐standing cylindrical columns under seismic excitation. *Earthquake Engineering & Structural Dynamics*. 2022;51(9):2016-35.

[40] R. Riddell. *Statistical analysis of the response of nonlinear systems subjected to earthquakes*. 1979: University of Illinois at Urbana-Champaign.

[41] J.A. Bachmann, M. Strand, M.F. Vassiliou , Broccardo M, Stojadinović B. Is rocking motion predictable?. *Earthq Eng Struct Dyn*. 2018; 47(2): 535-552.

[42] M.F. Vassiliou , M. Broccardo, C. Cengiz, M. Dietz, L. Dihoru, S. Gunay, K.M. Mosalam, G. Mylonakis, A. Sextos, B. Stojadinovic. Shake table testing of a rocking podium: Results of a blind prediction contest. *Earthq Eng Struct Dyn*. 2021; 50(4): 1043-1062.

[43] N. Reggiani Manzo, C.G. Lachanas, M.F. Vassiliou , D. Vamvatsikos. Uniform risk spectra for rocking structures. *Earthq Eng Struct Dyn*. 2022; 51(11): 2610-2626.

[44] A. Pappas, A. Sextos, Da Porto F, Modena C. Efficiency of alternative intensity measures for the seismic assessment of monolithic free-standing columns. *Bull Earthquake Eng*. 2017;15(4):1635-1659.

[45] B. Efron, R.J. Tibshirani. *An introduction to the bootstrap*. 1994: CRC press.